Electronic Supplementary Material (ESI) for Dalton Transactions.
This journal is © The Royal Society of Chemistry 2022

Supporting information

Ruthenium containing molecular electrocatalyst on glassy carbon for electrochemical water splitting

Lin Li,¥*[a,b,c] Biswanath Das,¥* [b] Ahibur Rahaman,[b] Andrey Shatskiy,[d] Fei Ye,[e] Peihong Cheng,[a] Chunze Yuan,[a,c] Zhiqi Yang,[a] Oscar Verho,*[b] Markus D. Kärkäs,[d] Joydeep Dutta,[e] Tsu-Chien Weng,[a,c] and Björn Åkermark*[b]

[a] Dr. L. Li, Dr. P. Cheng, Dr. C. Yuan, Z. Yang, and Prof. T. Weng
School of Physical Science and Technology, ShanghaiTech University, Shanghai 201210, China.
E-mail: lilin1@shanghaitech.edu.cn
[b] Dr. L. Li, Dr. B. Das, Dr. A. Rahaman, Dr. A. Shatskiy, Dr. O. Verho, and Prof. B. Åkermark
Department of Organic Chemistry, Arrhenius Laboratory Stockholm University, Svante Arrhenius v-g 16C, 10691 Stockholm, Sweden
E-mail: bjorn.akermark@su.se; oscar.verho@ilk.uu.se; Das.Biswanath85@gmail.com
[c] Dr. L. Li, Dr. C. Yuan, and Prof. T. Weng
Center for Transformative Science, ShanghaiTech University, Shanghai 201210, China
[d] Dr. A. Shatskiy, Prof. Markus D. Kärkäs
Department of Chemistry, KTH Royal Institute of Technology, Stockholm SE-100 44, Sweden.
[e] Dr. F. Ye, Prof. J. Dutta
Department of Applied Physics, Functional Materials, KTH Royal Institute of Technology, 106 91 Stockholm, Sweden

¥ Contributed equally to the project

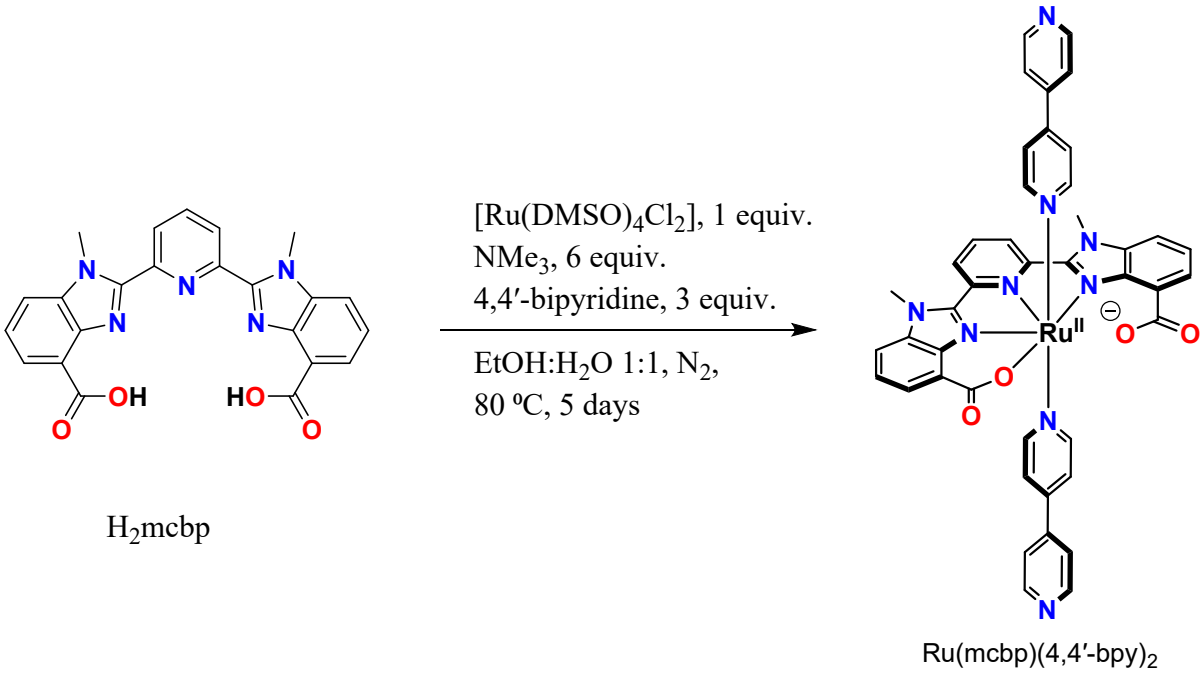

H_2mcbp

Scheme S1. Synthetic procedures of complex **2**.

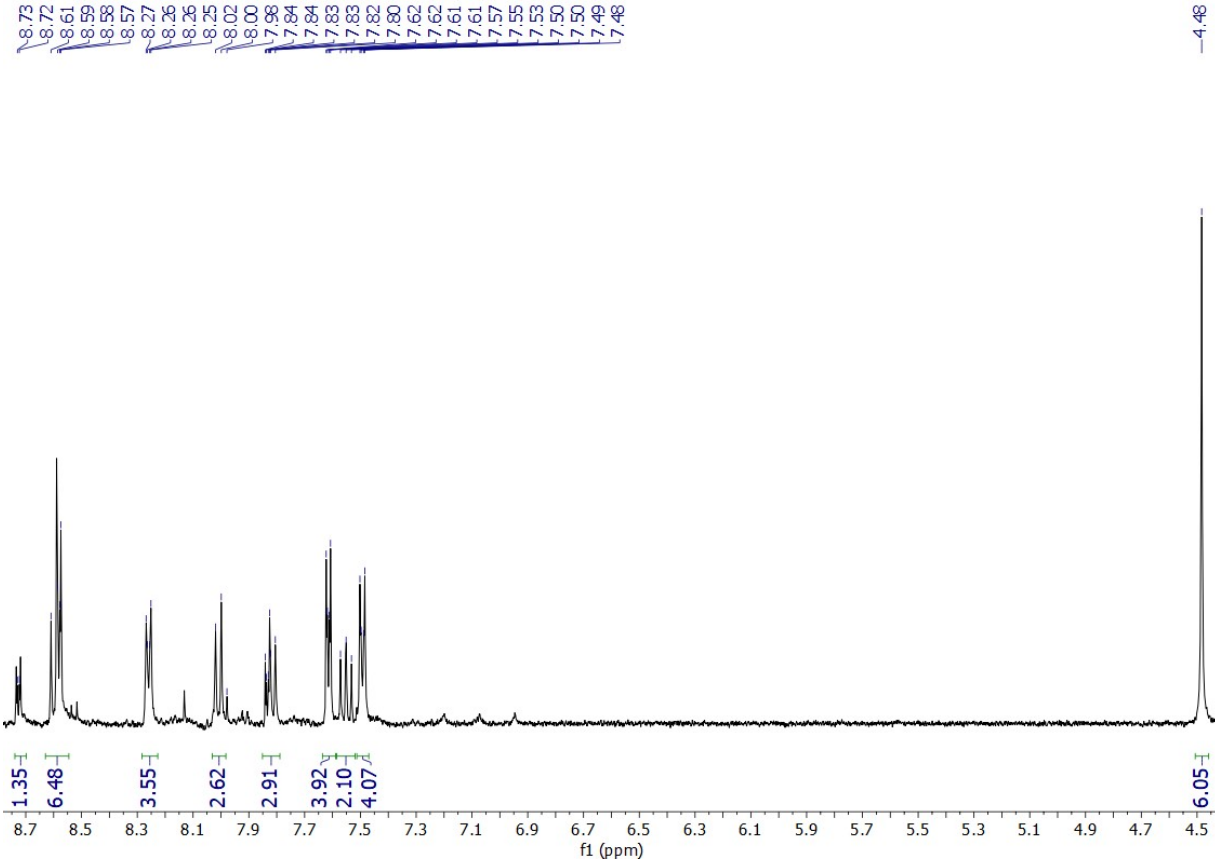

Figure S1. ^{1}H NMR (400 MHz, DMSO-d_6) of complex **2**.

^{1}H NMR (DMSO-d_6): δ 8.72 (dd, J = 6.2 and 2.8 Hz, 1H), 8.59 (m, 6H), 8.26 (dd, J = 7.0 and 3.5 Hz, 3H), 8.02 (d, J = 8.3 Hz, 2H), 7.83 (m, 3H), 7.61 (dd, J = 6.2 and 2.8 Hz, 4H), 7.53 (m, 2H), 7.49 (dd, J = 7.0 and 3.5 Hz, 4H), 4.48 (s, 6H, -CH_3 protons). ESI-HRMS: m/z 862.1424 ($C_{43}H_{31}N_9O_4Ru$ + Na, found), m/z 862.1446 (calculated).

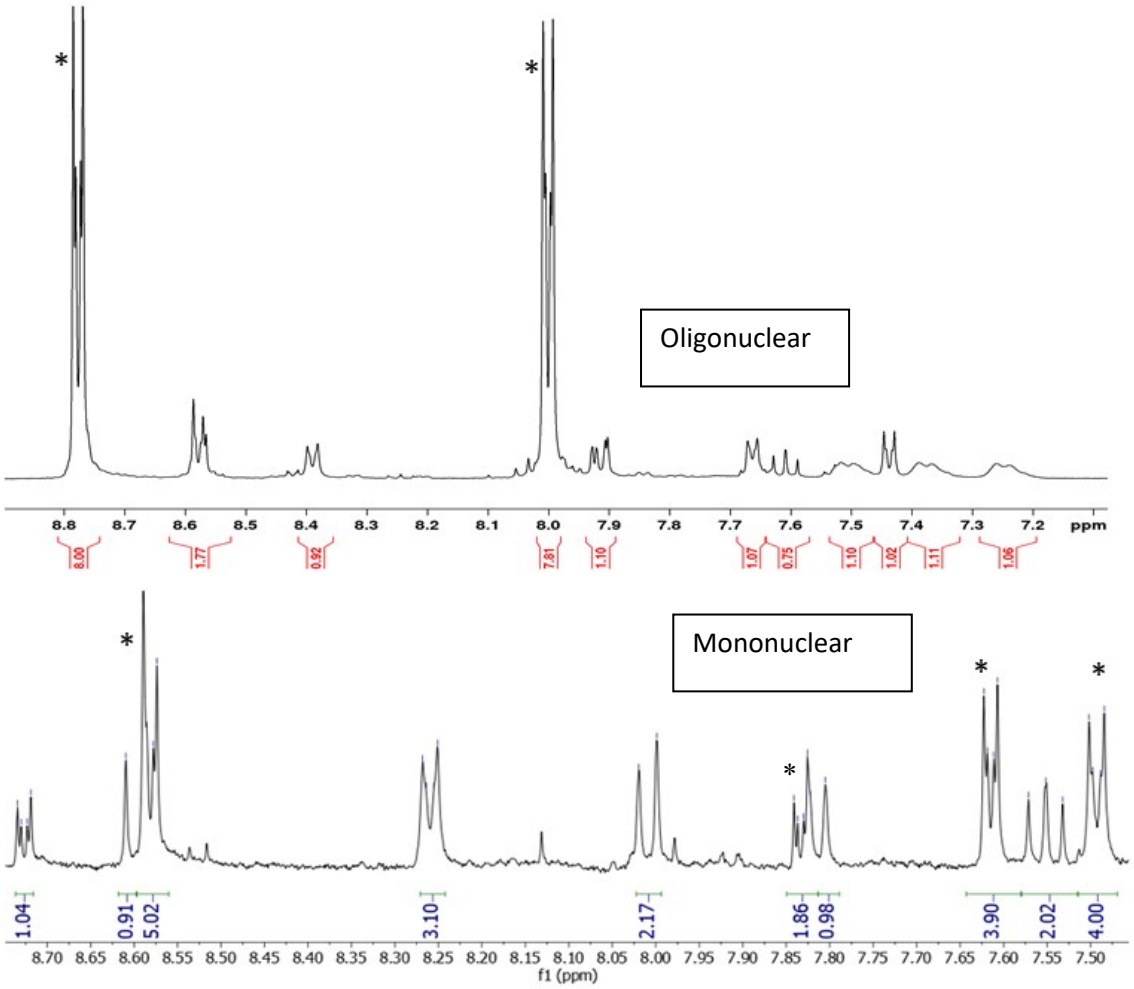

Figure S2. ^{1}H NMR comparison of the mononuclear and oligonulear complex in DMSO-d_6. * refers to the NMR signals from the bipyridine units.

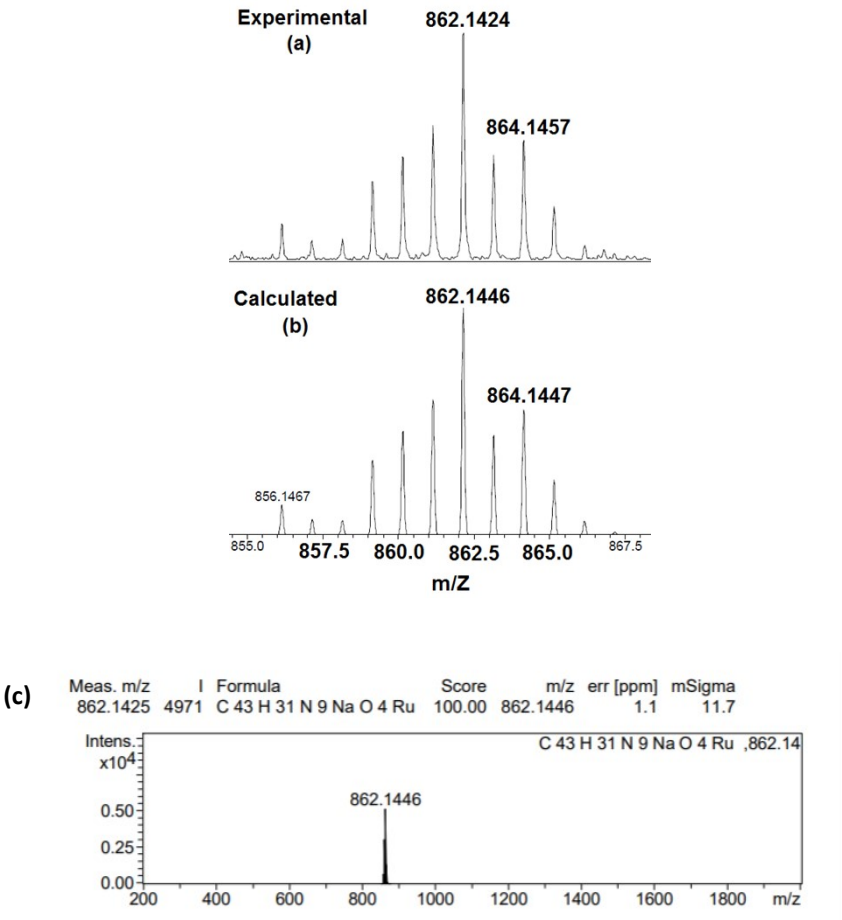

Figure S3. (a) Experimental isotope pattern of the major singly charged species at 862.1424, (b) corresponding calculated isotope pattern of the molecular formula $C_{43}H_{31}N_9O_4RuNa$ (**2**+Na^+), and (c) ESI-HRMS: Calculated for $C_{43}H_{31}N_9O_4NaRu$ $[M + Na]^+$: m/z 862.14, found: m/z 862.14. Err 1.1 ppm.

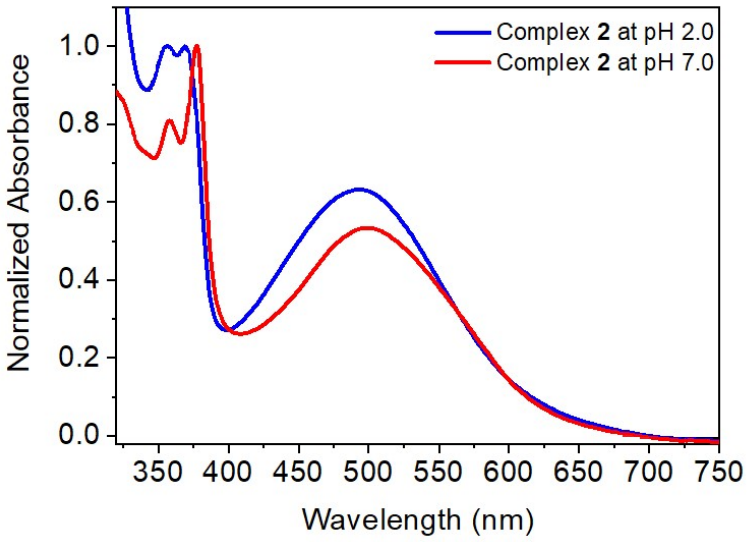

Figure S4. Normalized UV-vis spectra of **2** at pH 2.0 and pH 7.0. For the UV-Vis spectra of **1**, see reference 1.

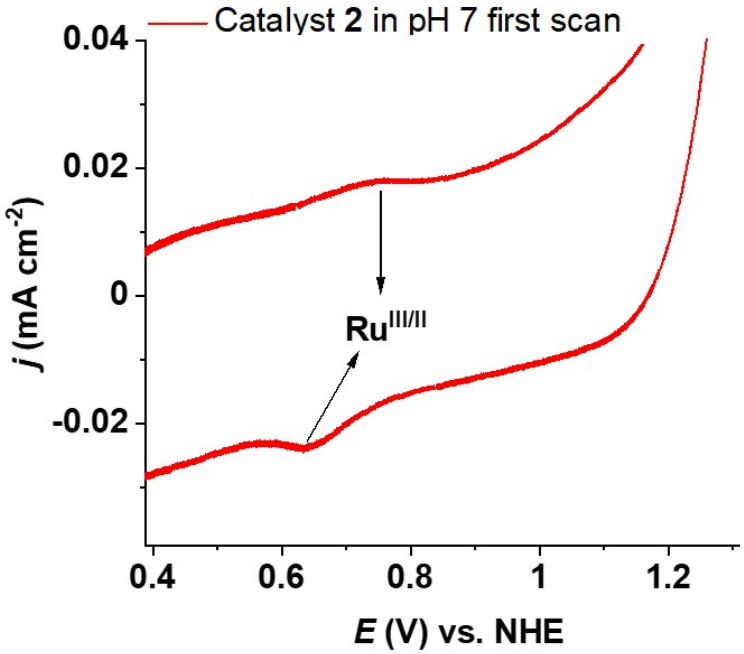

Figure S5. CV response of **2** at pH 7.0, in homogeneous condition, showing characteristic reversible $Ru^{III/II}$ redox wave at 0.69 V followed by water oxidation. $Ru^{IV/III}$ redox couple gets hidden under the WO catalytic wave. The scan rate was 100 mV/s. The working electrode (WE) was a glassy carbon disk. A Pt disk and an Ag/AgCl were used as counter electrode and reference electrode, respectively.

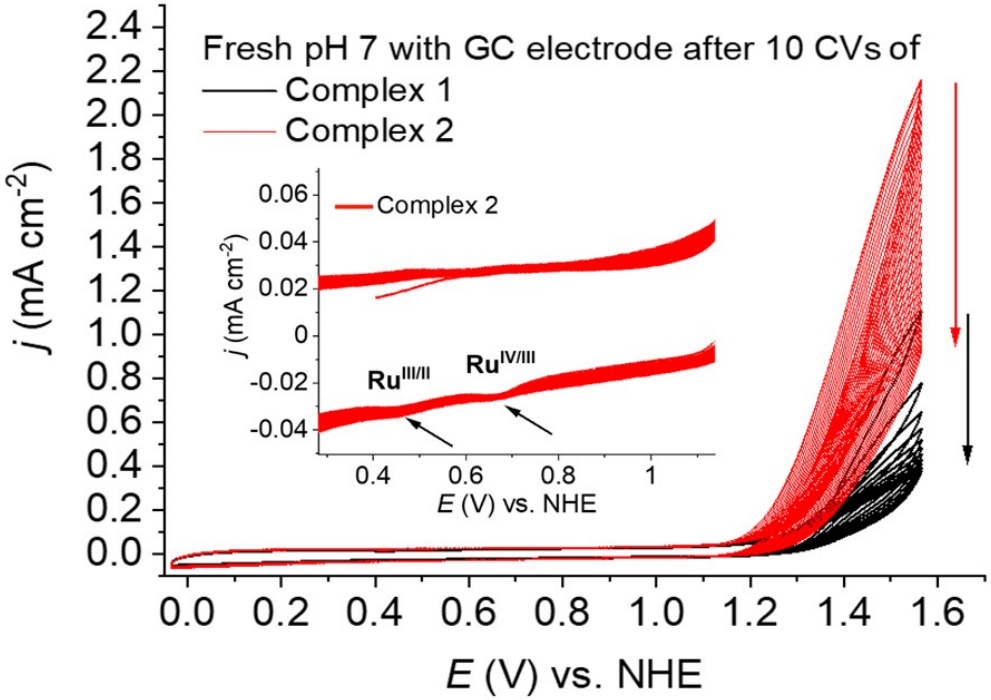

Figure S6. After 10 CV scans of 0.1 mM solutions of **1** and **2** (pH 7.0), the electrodes were removed, washed with water, and dried. These electrodes were reinvestigated at pH 7.0 without the presence of any catalysts. Inset is the zoomed-in (0.28 V to 1.12 V) redox response of complex **2** on the GC electrode. Characteristic $Ru^{III/II}$ (at 0.47 V) and $Ru^{IV/III}$ (at 0.68 V) redox waves confirm the molecular features of the catalyst. The scan rate was 100 mV/s. The working electrode (WE) was a glassy carbon disk. A Pt disk and an Ag/AgCl were used as counter electrode and reference electrode, respectively.

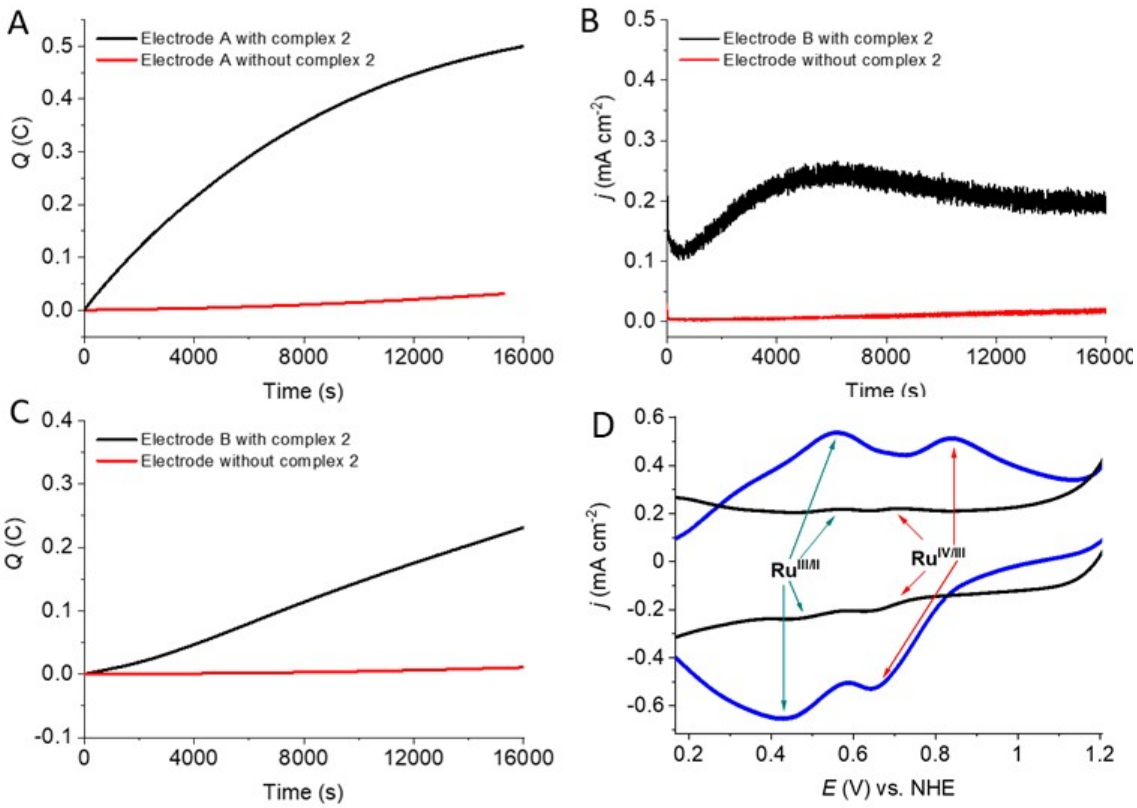

Figure S7. Bulk electrolysis using type A or type B electrodes with catalyst **2** as working electrode (black) and without catalyst **2** (red) in a phosphate-buffered solution at pH 7 at 1.4 V vs. NHE. (A) charge accumulation with time for electrode A, (B) change in current density over time for electrode B and (C) charge accumulation over time for electrode B. (D) (zoomed-in spectra of figure 3A of the manuscript) shows characteristic $Ru^{III/II}$ and $Ru^{IV/III}$ redox waves proving that molecular structure of catalyst **2** remains intact after immobilizing onto the glassy carbon electrode through MWCNTs.

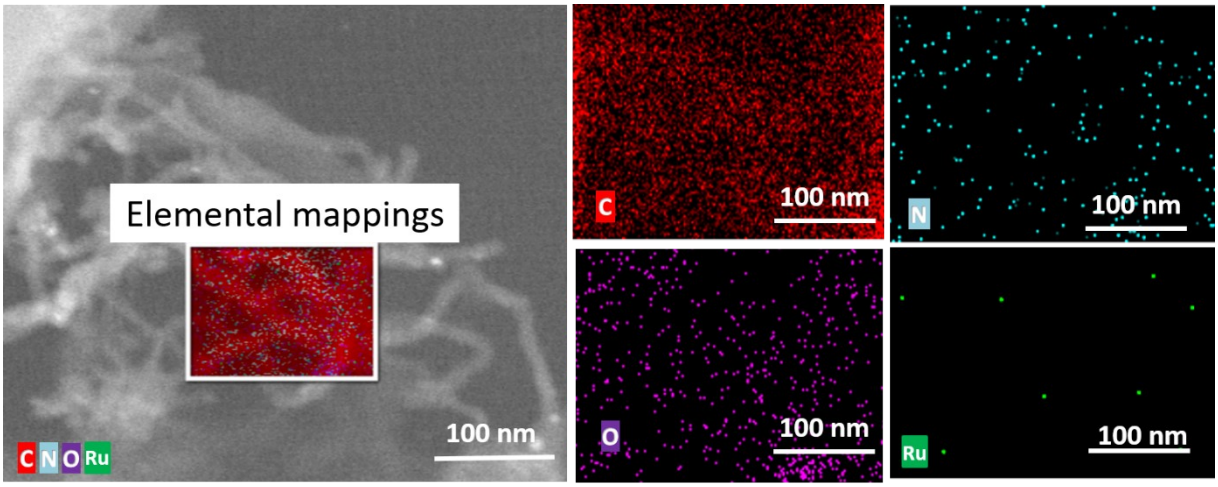

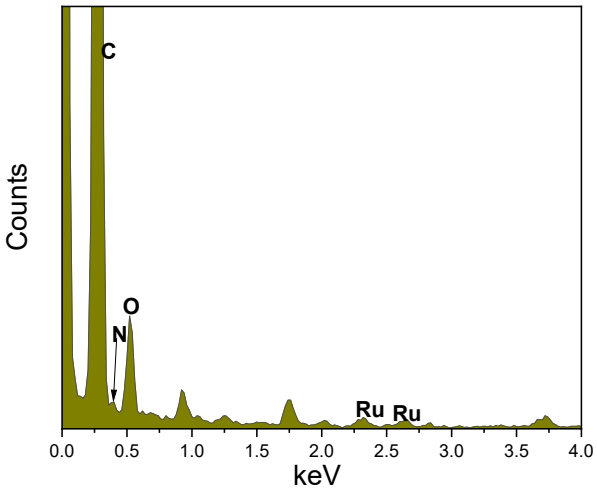

Figure S8. Scanning transmission electron microscopy (STEM) image of electrode type A with **2** and corresponding elemental mappings using energy dispersive X-ray spectroscopy (EDX).

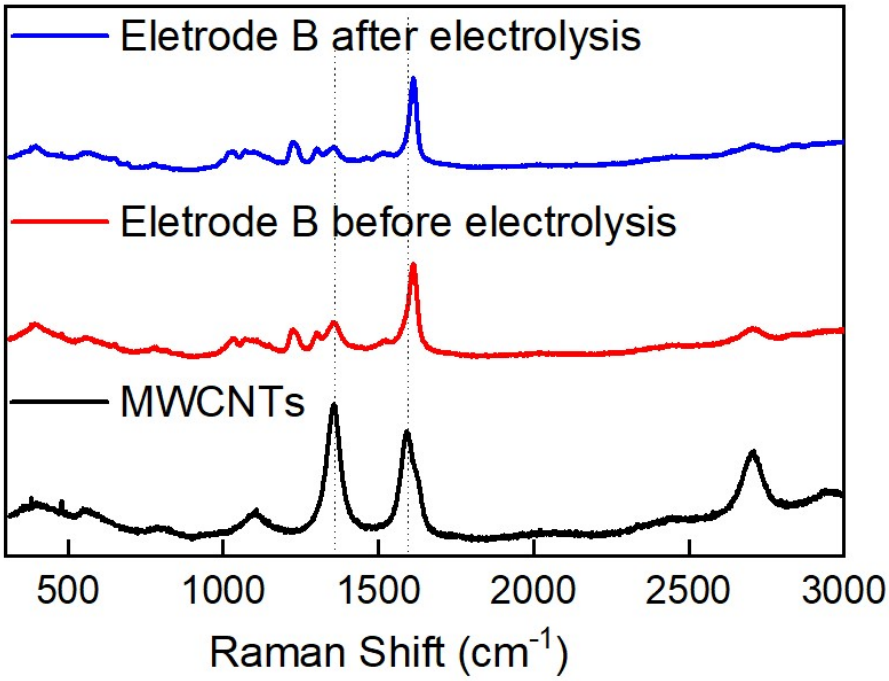

Figure S9. Raman spectral analysis of MWCNTs and electrode B with **2** before and after electrolysis.

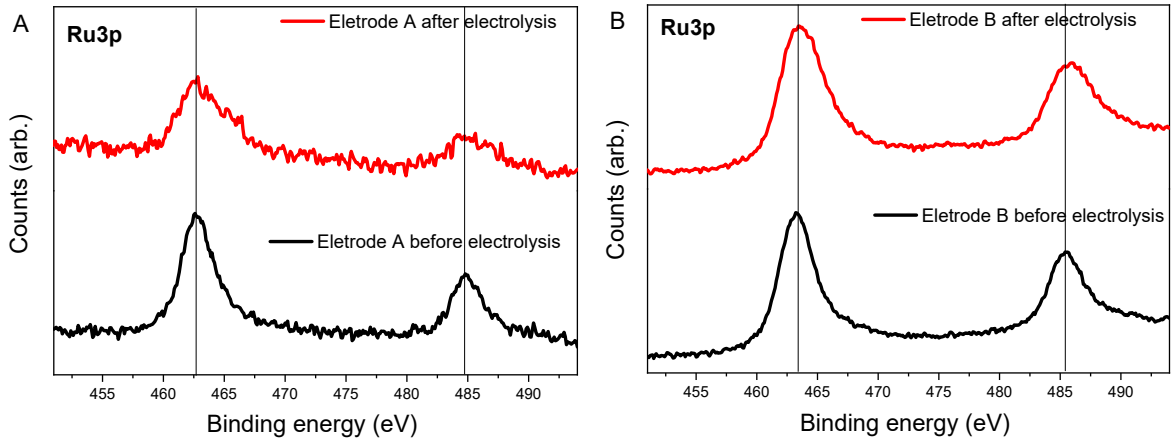

Figure S10. High-resolution XPS spectra for Ru 3p of (A) electrode A and (B) electrode B before and after electrolysis.

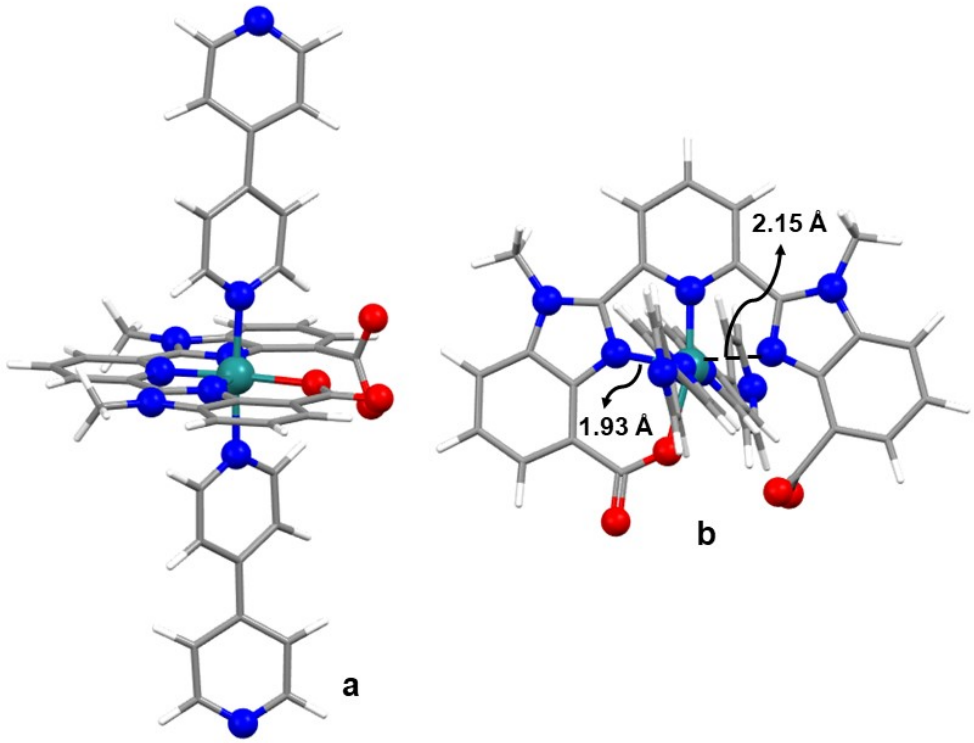

Figure S11. Two different orientations (a and b) of the fully optimized [by DFT, aqueous medium-SMD model, without any restriction] structure of **2** (cartesian coordinates are provided below) in aqueous medium. Blue, red, grey and turquoise colours represent nitrogen, oxygen, carbon and ruthenium atoms respectively. Two different Ru-N (benzimidazole) distances are depicted in Figure b.

Computational details: The standalone functional B97D3 (as implemented in the Gaussian09 package)[2] was used for the optimization of the geometries and for the calculation of the frequencies. The def2-TZVP basis set (and associated effective core potential) for the ruthenium atom and 6-31G(d,p) basis set for C, H, N and O atoms were used for the optimization.[3,4] Solvation effects were evaluated using the SMD model on the optimized geometries at the same level of theory as the geometry optimizations with water as the surrounding solvent.

Cartesian coordinates of the DFT optimized (unrestricted) geometry of **2** in aqueous medium

0 1 (Charge Multiplicity)

Ru	-0.00004000	-0.20056900	0.10254800
N	0.00007200	1.90721800	0.56831400

N	0.00025300	3.40968200	2.25539900
N	-0.00001000	-0.25056900	2.06225400
N	-0.00014800	-3.93909400	1.67675600
N	-0.00010000	-2.09697800	0.41341500
N	2.06241700	-0.13251600	-0.05311100
N	-2.06249600	-0.13240300	-0.05308600
O	-1.14428800	2.35956900	-2.99416400
O	1.14421500	2.35937400	-2.99433200
O	-0.00005800	-0.59390600	-1.97509500
O	-0.00017600	-1.83816400	-3.84433500
C	0.00017600	3.17856200	0.00566100
C	0.00017700	3.59328100	-1.34993300
C	0.00031600	4.98370700	-1.55789100
H	0.00032700	5.34478200	-2.58569700
C	0.00043500	5.91696400	-0.50426700
H	0.00053900	6.98211900	-0.73783100
C	0.00042600	5.51863400	0.83960100
H	0.00052100	6.24821100	1.64715100
C	0.00029500	4.13902500	1.06601600
C	0.00012500	2.06767300	1.92152200
C	0.00008600	0.91408600	2.79997700
C	0.00014600	0.84701200	4.20653500
H	0.00021900	1.74996400	4.80626400
C	0.00011600	-0.40339900	4.84153300
H	0.00016800	-0.45286800	5.92891700
C	0.00002700	-1.58669100	4.09139900
H	0.00002100	-2.55686500	4.58138700
C	-0.00004000	-1.50118300	2.69053400
C	-0.00011000	-2.54588000	1.68934100
C	-0.00013900	-4.34578400	0.32760900
C	-0.00015800	-5.58286400	-0.33260800
H	-0.00016500	-6.53558000	0.19448200
C	-0.00015600	-5.53479200	-1.73838600
H	-0.00016700	-6.47865000	-2.28338000
C	-0.00013600	-4.32568100	-2.47868900
H	-0.00013800	-4.33855400	-3.56694300
C	-0.00011200	-3.07941200	-1.83948800
C	-0.00011400	-3.15581000	-0.44265900
C	0.00002100	2.65541500	-2.56216900
C	0.00031900	3.99614400	3.58650300
H	-0.89701400	3.70144200	4.14584900
H	0.00034300	5.08365900	3.48434200
H	0.89767200	3.70139100	4.14579000
C	-0.00018000	-4.81078300	2.84050600
H	-0.00052300	-5.84936700	2.49902600
H	-0.89593300	-4.64403800	3.45403500
H	0.89585500	-4.64452200	3.45376200
C	-0.00009800	-1.74298600	-2.61337000
C	2.59465000	0.52583800	-1.11815700
H	1.90481300	1.00957000	-1.81648900
C	3.97229100	0.60504300	-1.30690400
H	4.33595000	1.17435400	-2.15946800
C	4.86083200	-0.00107900	-0.39903800
C	4.28541600	-0.67484700	0.69844600
H	4.90906900	-1.18952200	1.42701400
C	2.90297400	-0.71758300	0.83631200
H	2.43868200	-1.23749000	1.67043600
C	-2.59471600	0.52591400	-1.11816200
H	-1.90486500	1.00958700	-1.81651600
C	-3.97235600	0.60516800	-1.30689500

H	-4.33600300	1.17445300	-2.15948100
C	-4.86091100	-0.00086500	-0.39898400
C	-4.28550900	-0.67459300	0.69853300
H	-4.90917600	-1.18919700	1.42714000
C	-2.90306800	-0.71737900	0.83638500
H	-2.43878800	-1.23725400	1.67053500
C	-6.32689900	0.06428400	-0.58290400
C	-6.90541700	0.07284900	-1.86736200
C	-7.20785600	0.11880300	0.51525200
C	-8.29808500	0.13098800	-1.98671500
H	-6.28167300	0.00839500	-2.75753100
C	-8.58587300	0.17644100	0.28260200
H	-6.82442100	0.14654800	1.53456100
H	-8.75924400	0.13180300	-2.97728200
H	-9.27920700	0.22633400	1.12615700
C	6.32682000	0.06402000	-0.58297300
C	6.90532200	0.07263700	-1.86743800
C	7.20779400	0.11844100	0.51517400
C	8.29799100	0.13072800	-1.98680600
H	6.28156300	0.00825900	-2.75760300
C	8.58581000	0.17603900	0.28250900
H	6.82437300	0.14614200	1.53449000
H	8.75913700	0.13158200	-2.97737900
H	9.27915700	0.22585600	1.12605900
N	-9.14525200	0.18200500	-0.94145300
N	9.14517400	0.18165200	-0.94155300

References

[1] A. Shatskiy, A. A. Bardin, M. Oschmann, R. Matheu, J. Benet-Buchholz, L. Eriksson, M. D. Kärkäs, E. V. Johnston, C. Gimbert-Suriñach, A. Llobet, B. Åkermark, ChemSusChem 2019, 12, 2251-2262.

[2] S. Grimme, S. Ehrlich, L. Goerigk, Journal of Computational Chemistry 2011, 32, 1456-1465.

[3] F. Weigend, R. Ahlrichs, Physical Chemistry Chemical Physics 2005, 7, 3297-3305.

[4] M. J. Frisch, G. W. Trucks, H. B. Schlegel, G. E. Scuseria, M. A. Robb, J. R. Cheeseman, G. Scalmani, V. Barone, B. Mennucci, G. A. Petersson, H. Nakatsuji, M. Caricato, X. Li, H. P. Hratchian, A. F. Izmaylov, J.Bloino, G. Zheng, J. L. Sonnenberg, M. Hada, M. Ehara, K. Toyota, R. Fukuda, J. Hasegawa, M. Ishida, T. Nakajima, Y. Honda, O. Kitao, H. Nakai, T. Vreven, J. A. Montgomery, J. E. Peralta, F. Ogliaro, M. Bearpark, J. J. Heyd, E. Brothers, K. N. Kudin, V. N. Staroverov, R. Kobayashi, J. Normand, K. Raghavachari, A. Rendell, J. C. Burant, S. S. Iyengar, J. Tomasi, M. Cossi, N. Rega, J. M. Millam, M. Klene, J. E. Knox, J. B. Cross, V. Bakken, C. Adamo, J. Jaramillo, R. Gomperts, R. E. Stratmann, O. Yazyev, A. J. Austin, R. Cammi, C. Pomelli, J. W. Ochterski, R. L. Martin, K. Morokuma, V. G. Zakrzewski, G. A. Voth, P. Salvador, J. J. Dannenberg, S. Dapprich, A. D. Daniels, Farkas, J. B. Foresman, J. V. Ortiz, J. Cioslowski, D. J. Fox, Wallingford CT, 2009.